

Self-directed growth approach for acetylacetone lines on an H-terminated Si(001)-(2 × 1) surface

Jin-Ho Choi and Jun-Hyung Cho*

Department of Physics and Research Institute for Natural Sciences, Hanyang University, 17 Haengdang-Dong, Seongdong-Ku, Seoul 133-791, Korea

(Received 17 May 2011; published 29 July 2011)

We present theoretical investigations of the self-assembled growth of one-dimensional (1D) molecular lines directed across the dimer rows on the H-terminated Si(001)-(2 × 1) surface. Based on density-functional theory calculations, a growth approach of the 1D acetylacetone line is proposed, which involves the radical chain reaction initiated at two dangling-bond sites on one side of two adjacent Si dimers. It is also enabled that, if an H-free Si dimer were employed as the initial reaction site, a 1D acetylacetone line can grow along the dimer row. Our findings represent a novel insight into the growth of 1D molecular lines not only across but also along the dimer rows on the H-terminated Si(001)-(2 × 1) surface.

DOI: [10.1103/PhysRevB.84.035326](https://doi.org/10.1103/PhysRevB.84.035326)

PACS number(s): 68.43.Bc, 68.43.Fg, 68.43.Mn

I. INTRODUCTION

The fabrication of self-assembled organic nanostructures on a silicon surface has attracted much attention in recent years, because of its potential application for molecular electronic devices.¹⁻⁴ In particular, 1D molecular lines represent important building blocks for nanodevices. In their pioneering works, Lopinski *et al.*⁵ suggested the concept of self-directed growth to generate 1D molecular lines on the H-terminated Si(001)-(2 × 1) surface. However, there is a serious problem with the self-directed growth of molecular lines across the dimer rows, as discussed below. All of the previous studies with various alkene molecules, such as styrene,⁵⁻⁷ vinyl ferrocene,⁸ and long-chain alkenes (C_nH_{2n} ; $n \geq 8$) (Ref. 9) demonstrated the line growth only along the dimer rows, except with allyl mercaptan (ALM), $CH_2=CH-CH_2-SH$,¹⁰ which exhibited the line growth across the dimer rows. In this sense, for designing interconnected 1D molecular lines that connect two predefined positions on the Si(001)-(2 × 1) surface,^{11,12} a facile method for the line growth across the dimer rows is strongly demanded to be developed.

It is well established that the self-directed growth of 1D alkene lines along the dimer rows occurs via the so-called radical chain reaction mechanism.⁵⁻⁹ By creating a dangling bond (DB) at the H-terminated Si(001)-(2 × 1) surface using the tip of a scanning tunneling microscope (STM) (Refs. 3 and 13) and exposing it to alkene vapor, the C- π bond of alkene reacts with the created DB to form a C-centered radical. Subsequently, the created C-centered radical is stabilized by the abstraction of an H atom from a neighboring Si-H site, thereby generating a new DB that sets off a chain reaction along the dimer row [see the line A in Fig. 1(a)]. In contrast, the self-directed growth of ALM line^{10,11} across the dimer rows involves several reaction processes:¹⁴ (i) the created radical at the C atom is transferred to the S atom, (ii) the resulting S-centered radical easily abstracts an H atom from the neighboring dimer row, and (iii) the generated S-H group further reacts with the neighboring dimer row to produce the Si-S bond on the neighboring dimer row, accompanying the associative desorption of H_2 . This H_2 -desorption process creates a new DB on the neighboring dimer row, setting off the chain reaction across the dimer rows [see the line B in Fig. 1(a)]. Because of such rather complicated reaction

processes during the ALM line growth,¹⁴ the employed radical chain reaction mechanism has so far been uniquely applicable to ALM molecule.^{10,11}

In this paper, we present a radical chain reaction mechanism that produces a facile self-directed growth of 1D molecular lines across the dimer rows on the H-terminated Si(001)-(2 × 1) surface. The essence of this mechanism lies in the use of two DBs on one side of two adjacent Si dimers as the reaction site [marked with X_1 in Fig. 1(a)] instead of a previously¹⁰ employed single DB. To react with the two DBs, we chose the keto form of the acetylacetone (ACA) molecule, $CH_3-CO-CH_2-CO-CH_3$,¹⁵ containing two carbonyl groups [see the inset of Fig. 1(a)]. A single ACA molecule adsorbs on the created two DBs, forming two Si-O bonds and two C radicals. Such a radical intermediate easily abstracts two H atoms from the other side of the reacted dimers, leaving two new DBs. The second ACA molecule can attach at the created two DBs, proceeding to abstract two H atoms from the neighboring dimer row. The achievement of the two consecutive H-abstraction processes on the reacted dimers and from the neighboring dimer row allows the chain reaction for an ACA line across the dimer rows [see Fig. 1(b)]. In addition, we find that, if an H-free dimer (generated by the removal of two H atoms on an H-passivated dimer using the STM tip¹⁶) were used as the initial reaction site [marked with X_2 in Fig. 1(a)], the radical chain reaction is also facilitated to form an ACA line along the dimer row [see Fig. 1(c)]. Thus, the growth direction of the ACA line can be controlled to be not only across but also along the dimer rows on the H-terminated Si(001)-(2 × 1) surface by employing the two different types of reaction sites.

II. CALCULATIONAL METHOD

We performed the total-energy calculations by using first-principles density-functional theory¹⁷ within the generalized-gradient approximation.¹⁸ The Si and H (C and O) atoms are described by norm-conserving¹⁹ (ultrasoft²⁰) pseudopotentials. The surface is modeled by a periodic slab geometry. Each slab contains six Si atomic layers, where ACA molecules adsorb on top of the slab and the bottom Si layer is passivated by two H atoms per Si atom. The electronic wave functions

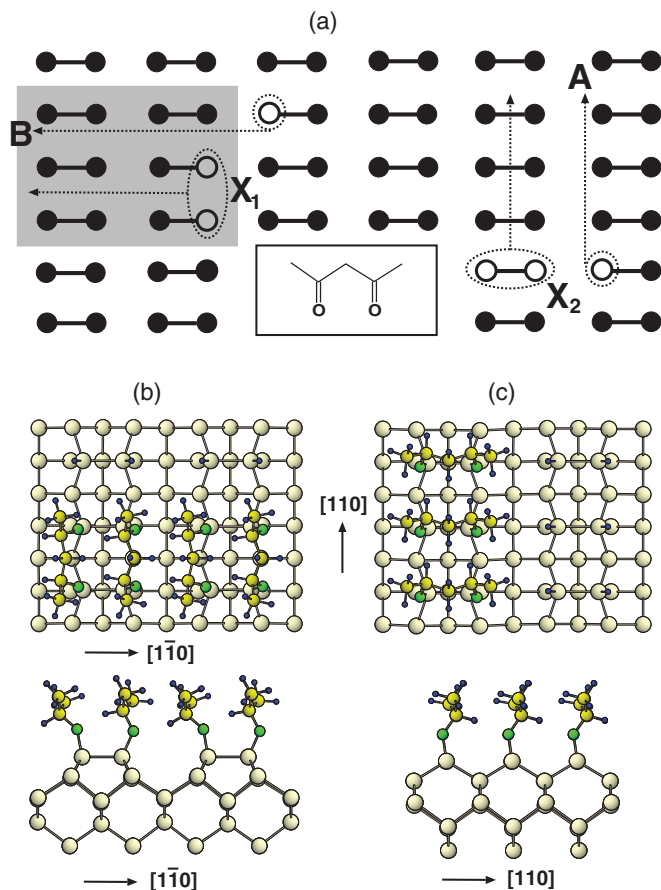


FIG. 1. (Color online) (a) Schematic top view of a dimerized Si(001)-(2 × 1) surface. Top and side views of the optimized structure of an ACA molecular line (b) across the dimer rows and (c) along the dimer row are shown. A (B) represents the line growth along (across) the dimer rows. The keto form of ACA molecule is schematically drawn in the inset of (a). (a) The filled (open) circles represent H-bonded (bare) Si atoms. (b) and (c) The circles represent Si, C, O, and H atoms with decreasing size.

are expanded in a plane-wave basis set using a cutoff of 25 Ry, and the electron density is obtained from the wave functions at four \mathbf{k} points in the surface Brillouin zone of the 4×3 unit cell. All the atoms except the bottom two Si layers are allowed to relax along the calculated Hellmann-Feynman forces until all the residual force components are less than 1 mRy/bohr. Our calculation scheme has been successfully applied for the adsorption and reaction of various unsaturated hydrocarbon molecules on Si(001)-(2 × 1).^{14,21}

III. RESULTS

First, we study the reaction of an ACA molecule with two DBs generated on one side of two adjacent dimers on an otherwise H-terminated Si(001)-(2 × 1) surface. In our calculations, this reaction is simulated by employing a 4×3 unit cell [see the highlighted area in Fig. 1(a)]. The two π bonds of carbonyl groups interact with two DBs, forming two Si–O bonds and two C radicals.²² We find that such a C radical intermediate (denoted as R_0) has an adsorption energy (E_{ads}) of -0.75 eV. As shown in the inset of Fig. 2(a), our optimized

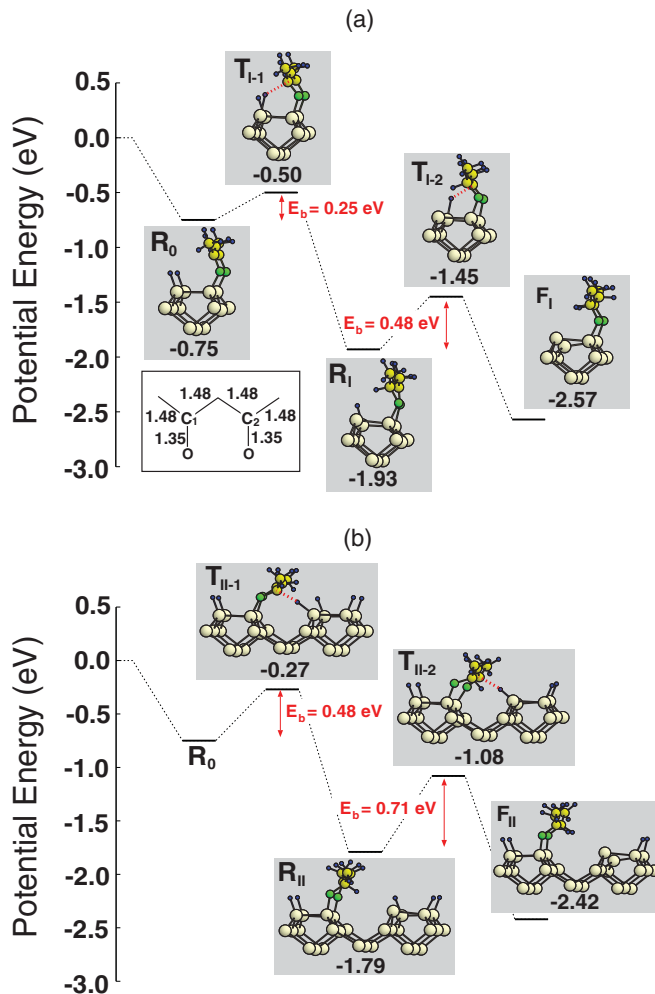


FIG. 2. (Color online) Calculated energy profiles along the H-abstraction pathways (a) I and (b) II. The atomic geometries of the intermediate (R), transition (T), and final (F) states are given together with their adsorption energies (in eV). The energy barriers for two H-abstraction steps are also given. The bond lengths (in Å) of the R_0 state are given.

structure of the R_0 state shows that the C_1 and C_2 atoms are bonding not only to two neighboring C atoms with an identical C–C bond length (1.48 Å) but also to one O atom with a C–O bond length of 1.35 Å. This fact clearly indicates that there are two radicals at the C_1 and C_2 atoms, rather than pairing of the two radical electrons.

Similar to the cases of the self-directed growth of alkene lines,^{5–9} the produced C radicals in the R_0 state can be stabilized by the abstraction of H atoms from either the other side of the reacted dimers (labeled as the H-abstraction pathway I) or a neighboring dimer row (labeled as the H-abstraction pathway II). In order to find the minimum-energy pathway for such H-abstraction processes, we optimize the structure by using the gradient projection method²³ where only the distance $d_{\text{C-H}}$ between a C radical atom and an abstracted H atom is constrained. Therefore, we obtain the energy profile for the H-abstraction pathway as a function of decreasing distance $d_{\text{C-H}}$. Figures 2(a) and 2(b) show the calculated energy profiles along the H-abstraction pathways I and II,

respectively, together with the atomic geometries of the intermediate (R), transition (T), and final (F) states. There are two H-abstraction steps because of the presence of two C radicals. Along the pathway I, the transition state (T_{I-1}) for the first H abstraction has $E_{\text{ads}} = -0.50$ eV, yielding an energy barrier (E_b) of 0.25 eV from R_0 to the intermediate state (R_I) in which one C radical remains. Subsequently, R_I with $E_{\text{ads}} = -1.93$ eV proceeds to undergo the second H abstraction, where the transition state (T_{I-2}) has $E_{\text{ads}} = -1.45$ eV, yielding $E_b = 0.48$ eV from R_I to the final state (F_I). Using an Arrhenius-type activation equation with a typical value of $\sim 10^{13}$ Hz for the pre-exponential factor,²⁴ we estimate that at room temperature, the reaction rate for the first (second) H-abstraction is $\sim 6.4 \times 10^8$ (8.9×10^4) s^{-1} , indicating an easily activated reaction. We note that the reverse reaction from the F_I (R_I) to the R_I (R_0) states has $E_b = 1.43$ (1.12) eV, hardly occurring at room temperature.

Along the pathway II, the barriers for the H abstraction are expected to be higher than those along the pathway I because of a relatively longer distance between the C radical atom and the abstracted H atom. As shown in Fig. 2(b), the first (second) H abstraction at the R_0 (R_{II}) state takes place with a relatively higher barrier of $E_b = 0.48$ (0.71) eV, compared to the corresponding one (0.25 and 0.48 eV for the first and the second H abstraction, respectively) along the pathway I. Thus, we estimate that at room temperature, the H abstraction through the path I is $\sim 7.2 \times 10^3$ times more easily activated than that through the path II. We note that along the path II, the intermediate (final) state, R_{II} (F_{II}), with $E_{\text{ads}} = -1.79$ (-2.42) eV is less stable than R_I (F_I) along the path I by 0.14 (0.15) eV. Consequently, the H abstraction from the other side of the reacted dimers (path I) is kinetically and thermodynamically facilitated compared to that from a neighboring dimer row (path II), leading to formation of the F_I state.

To achieve the chain reaction across the dimer rows, the second ACA molecule adsorbing on the DB sites of the F_I state should succeed to abstract two H atoms from a neighboring dimer row. The calculated energy profile for this H abstraction is displayed in Fig. 3, together with the atomic geometries of various states. We find that the C radical intermediate (R_{S-0} in Fig. 3) has $E_{\text{ads}} = -0.43$ eV which is smaller in magnitude than that (-0.75 eV) of the first ACA molecule at the R_0 state. The less stability of R_{S-0} indicates that there exists a repulsive intermolecular interaction between two adsorbed molecules. As shown in Fig. 3, the first (second) H abstraction occurs via the transition state T_{S-1} (T_{S-2}) with $E_b = 0.35$ (0.70) eV. The Arrhenius analysis for the first (second) H-abstraction gives a rate of $\sim 1.4 \times 10^7$ (~ 18) s^{-1} at room temperature. These H-abstraction steps stabilize the intermediate (R_{S-1}) and final (F_S) states with $E_{\text{ads}} = -1.67$ and -2.41 eV, respectively. Considering that the reverse reaction from F_S to R_{S-1} or R_{S-0} is hardly expected to occur because of high activation barriers, it is most likely that the second ACA molecule attains formation of the F_S state through H abstraction, thereby allowing the chain reaction for an ACA line across the dimer rows.

A recent STM study of Hossain *et al.*¹¹ reported that interconnected 1D molecular lines connecting two predefined positions on the H-terminated Si(001)-(2 × 1) surface can be fabricated with the two different molecules, i.e., styrene and ALM, which undergo the radical chain reaction along and

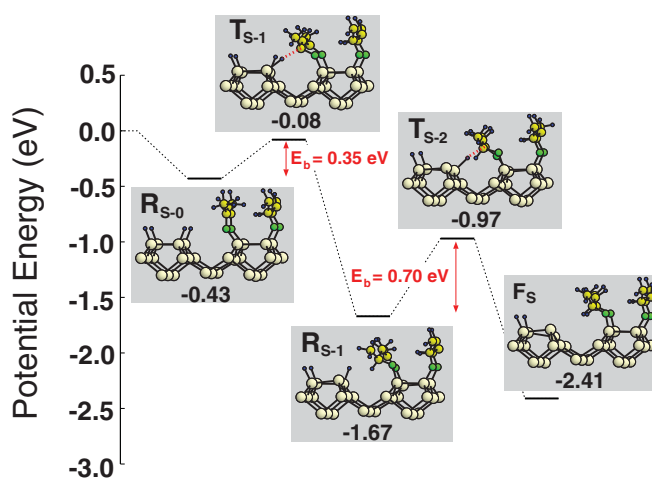


FIG. 3. (Color online) Calculated energy profile of H-atom abstraction for the second adsorbed ACA across the dimer rows.

across the dimer rows, respectively. Using a single molecule (i.e., acetophenone), Hossain *et al.* also reported the self-assembled growth of interconnected 1D molecular lines, which cannot however connect two predefined positions.¹² Here, we demonstrate that an ACA line can also grow along the dimer row, if an H-free dimer were employed as the reaction site. Figure 4 shows the calculated energy profile of the two H-abstraction steps for an ACA molecule adsorbed on the H-free dimer. We find that the radical intermediate R_{H-0} with $E_{\text{ads}} = -0.53$ eV easily undergoes the first H abstraction with $E_b = 0.05$ eV, much smaller than the corresponding ones across the dimer rows. For the second H-abstraction step on going from R_{H-1} to the F_H state (see Fig. 4), we obtain $E_b = 0.55$ eV, giving rise to an estimated reaction rate of $\sim 6.0 \times 10^3$ s^{-1} at room temperature. We note that, when comparing the energy profiles of H-atom abstraction between across the dimer rows [Fig. 2(a)] and along the dimer row (Fig. 4), the initial intermediate states (R_0 and R_{H-0}) show a large adsorption energy difference of 0.22 eV, while other states show a small deviation of adsorption energy ranging from 0.01 to 0.06 eV. As a result, the energy barrier ($E_b = 0.25$ eV) on going from R_0 to R_I is larger than that ($E_b = 0.05$ eV) on going from R_{H-0}

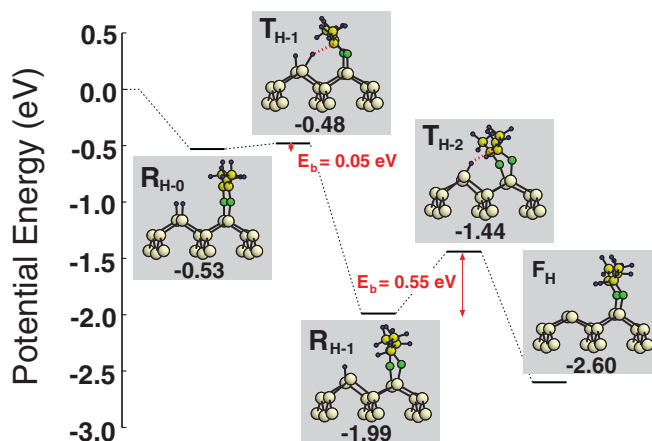


FIG. 4. (Color online) Calculated energy profile of H-atom abstraction along the dimer row.

TABLE I. Calculated adsorption energies (in eV) of the intermediate and transition states as well as energy barriers during various H-abstraction processes [shown in Figs. 2(a), 3, and 4] for ACA and MACA.

		$R_0 \rightarrow T_{1-1}$	$R_1 \rightarrow T_{1-2}$	$R_{S-0} \rightarrow T_{S-1}$	$R_{S-1} \rightarrow T_{S-2}$	$R_{H-0} \rightarrow T_{H-1}$	$R_{H-1} \rightarrow T_{H-2}$
ACA	E_{ads}	-0.75, -0.50	-1.93, -1.45	-0.43, -0.08	-1.67, -0.97	-0.53, -0.48	-1.99, -1.44
	E_b	0.25	0.48	0.35	0.70	0.05	0.55
MACA	E_{ads}	-0.66, -0.42	-1.98, -1.55	-0.27, +0.03	-1.68, -0.94	-0.38, -0.35	-2.03, -1.50
	E_b	0.24	0.43	0.30	0.74	0.03	0.53

to R_{H-1} . These subtle differences along the two growth directions possibly arise from the fact that the reaction site X_2 [see Fig. 1(a)] is energetically more stable than X_1 by 0.16 eV.²⁵

The radical chain reaction mechanism presented here can be applicable to other organic molecules containing two carbonyl groups, such as methylacetylacetone (MACA), 3-phenylacetylacetone, and 3-chloroacetylacetone, where one H atom bonded to the center C atom of the ACA molecule is substituted with the methyl group, phenyl group, and Cl atom, respectively. For MACA, we calculated the adsorption energies of the intermediate and transition states as well as energy barriers during various H-abstraction processes, in comparison with those for ACA (see Table I). We find that the results for MACA and ACA are close to each other, showing that the line growth not only across but also along the dimer rows can be available for ACA's isostructural molecules.

IV. SUMMARY

In summary, we have presented a facile method for the growth of 1D molecular lines directed not only across but also along the dimer rows on the H-terminated Si(001)-(2 × 1) surface. We showed that the two different types of initial reaction sites determine the growth direction of the ACA line. The present method will shed more light on the fabrication of interconnected 1D molecular lines connecting two predefined positions on the H-terminated Si(001)-(2 × 1) surface.

ACKNOWLEDGMENTS

This work was supported by National Research Foundation of Korea (NRF) grant funded by the Korean Government (NRF-2011-0015754).

*chojh@hanyang.ac.kr

¹C. P. Poole Jr. and F. J. Owens, *Introduction to Nanotechnology* (Wiley, NY, 2003) and references therein.

²R. A. Wolkow, *Annu. Rev. Phys. Chem.* **50**, 413 (1999).

³M. A. Walsh and M. C. Hersam, *Annu. Rev. Phys. Chem.* **60**, 193 (2009).

⁴K. A. Perrine and A. V. Teplyakov, *Chem. Soc. Rev.* **39**, 3256 (2010).

⁵G. P. Lopinski, D. D. M. Wayner, and R. A. Wolkow, *Nature* **406**, 48 (2000).

⁶J.-H. Cho, D. H. Oh, and L. Kleinman, *Phys. Rev. B* **65**, 081310 (2002).

⁷J. K. Kang and C. B. Musgrave, *J. Chem. Phys.* **116**, 9907 (2002).

⁸P. Kruse, E. R. Johnson, G. A. DiLabio, and R. A. Wolkow, *Nano Lett.* **2**, 807 (2002).

⁹G. A. DiLabio, P. G. Piva, P. Kruse, and R. A. Wolkow, *J. Am. Chem. Soc.* **126**, 16048 (2004).

¹⁰Md. Z. Hossain, H. S. Kato, and M. Kawai, *J. Am. Chem. Soc.* **127**, 15030 (2005).

¹¹Md. Z. Hossain, H. S. Kato, and M. Kawai, *J. Phys. Chem. B* **109**, 23129 (2005).

¹²Recent STM experiment [Hossain *et al.*, *J. Am. Chem. Soc.* **130**, 11518 (2008)] observed that acetophenone exhibited the line growth either along the dimer row or across the dimer rows. However, the growth direction of acetophenone lines cannot be controlled because it is randomly determined.

¹³T.-C. Shen, C. Wang, G. C. Abeln, J. R. Tucker, J. W. Lyding, Ph. Avouris, and R. E. Walkup, *Science* **268**, 1590 (1995).

¹⁴J.-H. Choi and J.-H. Cho, *Phys. Rev. Lett.* **102**, 166102 (2009).

¹⁵There are the ACA crystals with the di-keto and enol forms, separating the two forms [Johnson *et al.*, *J. Chem. Phys.* **116**, 5694 (2001)]. After evaporation of crystalline di-keto ACA, the di-keto form remains because its conversion to the enol form was estimated to be activated with a high energy barrier of ~2.6 eV [see G. Alagona and C. Ghio, *Int. J. Quantum Chem.* **108**, 1840 (2008)].

¹⁶X. Tong and R. A. Wolkow, *Surf. Sci. Lett.* **600**, L199 (2006).

¹⁷P. Hohenberg and W. Kohn, *Phys. Rev.* **136**, B864 (1964); W. Kohn and L. J. Sham, *ibid.* **140**, A1133 (1965).

¹⁸J. P. Perdew, K. Burke, and M. Ernzerhof, *Phys. Rev. Lett.* **77**, 3865 (1996); **78**, 1396(E) (1997).

¹⁹N. Troullier and J. L. Martins, *Phys. Rev. B* **43**, 1993 (1991).

²⁰D. Vanderbilt, *Phys. Rev. B* **41**, 7892 (1990); K. Laasonen, A. Pasquarello, R. Car, C. Lee, and D. Vanderbilt, *ibid.* **47**, 10142 (1993).

²¹J.-H. Choi and J.-H. Cho, *J. Am. Chem. Soc.* **128**, 11340 (2006); J.-H. Cho and L. Kleinman, *Phys. Rev. B* **71**, 125330 (2005); H. J. Kim and J.-H. Cho, *J. Chem. Phys.* **120**, 8222 (2004).

²²It is well known experimentally and theoretically that the initial interaction of organics containing carbonyl group with the Si(001) surface produces the Si-O bond formation, showing that the lone pair of the O atom is attracted to the Si atom. For instance, in the adsorption of acetone on Si(001), the precursor state is produced by forming a Si-O bond, indicating that the lone-pair state of the O atom hybridizes with the empty dangling-bond state of the Si atom [see Schofield *et al.*, *J. Am. Chem. Soc.* **129**, 11402 (2007); Lee *et al.*, *J. Chem. Phys.* **129**, 194110 (2008)]. In the case of ACA, it is noteworthy that H-dissociation after a single Si-O bond formation may be possible. However, this H-dissociation is

an activated process with an energy barrier [Lee *et al.*, *J. Chem. Phys.* **129**, 194110 (2008)] whereas the formation process of the R_0 state is barrierless [similar to an example of *O*-phthalaldehyde: Choi and Cho, *Phys. Rev. Lett.* **98**, 246101 (2007)]. Thus, it is most likely that the formation of R_0 is kinetically favored over the H-dissociation process.

²³D. A. Wismer and R. Chatterly, *Introduction to Nonlinear Optimization* (North-Holland, Amsterdam, 1978), pp. 174–178. Our gradient projection method obtained an energy barrier of 0.02 eV for ethylene adsorption from the precursor state to the final state [*Phys. Rev. B* **69**, 075303 (2004)], close to that (0.06 eV) obtained by the nudged elastic band method [Fan *et al.*, *Phys. Rev. B* **72**, 165305 (2005)]. For the reaction pathway of 1D styrene line, our gradient projection method obtained an energy barrier of 0.88 eV (Ref. 6), comparable with 0.76 eV (Ref. 7) and 1.05 eV (Ref. 5).

²⁴Steric factor of ACA (reducing pre-exponential factor) may significantly reduce the formation rate of the ACA line. However, using $\sim 10^{13}$ Hz pre-exponential factor, we predicted the self-

directed growth of *o*-phthalaldehyde line on H-terminated Si(001)-(2 × 1) [Choi and Cho, *Phys. Rev. Lett.* **98**, 246101 (2007)], which was subsequently confirmed by a recent STM experiment [Walsh and Hersam, *Chem. Commun.* **46**, 1153 (2010)].

²⁵It is well known that two DBs placed on one side of two adjacent Si dimers [X_1 in Fig. 1(a)] are less stable than those placed on the same Si dimer [X_2 in Fig. 1(a)] (see Ref. 25). In our calculations, the reaction site X_1 [see Fig. 1(a)] is energetically less stable than X_2 by 0.16 eV. The energy difference between these two kinds of DB configurations is termed “pairing energy” [Höfer *et al.*, *Phys. Rev. B* **45**, 9485 (1992)]. Considering the fact that two DBs are saturated by the molecular adsorption in the R_0 and R_{H-0} states, the adsorption energy difference between the R_0 and R_{H-0} states possibly arises from the different stability of the two kinds of DB configurations. However, other states after the initial intermediate state undergo H-abstraction processes, thereby creating DB(s). Thus, the adsorption energy difference between the corresponding other states on Fig. 2(a) and Fig. 4 becomes relatively reduced compared to the case of the initial intermediate states (R_0 and R_{H-0}).